The Mechanical Properties of Insert-Molded Bimaterial Composites: Series and Parallel Geometries

C. W. EXTRAND, S. BHATT

Entegris, 3500 Lyman Boulevard, Chaska, Minnesota 55318

Received 4 June 1999; accepted 19 September 1999

ABSTRACT: Series and parallel bimaterial composites were constructed by injecting C fiber poly(ether ether ketone) (PEEK) into a mold containing a fraction of a previously molded polycarbonate (PC) dogbone. Resulting specimens were tested in tension. For series composites, breaking stresses were independent of fractional length. However, elongation to break decreased with fractional length of C fiber PEEK and apparent stiffness increased. On the other hand, for parallel composites, breaking strains were independent of the fractional cross-sectional area, while breaking stress and stiffness increased with the C fiber PEEK fraction. © 2000 John Wiley & Sons, Inc. J Appl Polym Sci 76: 1777–1784, 2000

Key words: insert-mold; over-mold; bimaterial; composite; mechanical; stress; strain; modulus

INTRODUCTION

Insert molding involves injecting a polymer over another material.[1,2] This approach marries the best features of different materials and provides an economical method for producing higher-performance products at a reduced cost. In some cases, it is a good alternative to polymer blends. An important consideration for any insert-molded product is the mechanical performance of the resulting bimaterial composite. However, very little has been published in this area.[1]

Thus, in this study, the mechanical properties of insert-molded bimaterial composites were examined. Series and parallel composite specimens were constructed by injecting C fiber poly(ether ether ketone) (PEEK) into a mold containing a fraction of a polycarbonate (PC) dogbone to create a thermophysical bond. The resulting specimens were tested in tension and analyzed. The mechanical properties of the two specimen geometries were compared.

Correspondence to: C. Extrand (chuck_extrand@entegris.com).

Journal of Applied Polymer Science, Vol. 76, 1777–1784 (2000)

ANALYSIS

Apparent Stresses and Strains

A detailed analysis of the stress field near the interface of a bimaterial composite was examined previously.[3–9] In this study, the stress field in the immediate vicinity of the interface was neglected. Our aim was to understand the apparent or far-field mechanical response of series and parallel bimaterial composites. The approach used to analyze our findings is given below.

The apparent tensile stress (σ) of monolithic or composite specimens was calculated using the elongation force (F) divided by its initial or undeformed cross-sectional area (A) [10,11]:

$$\sigma = F/A \quad (1)$$

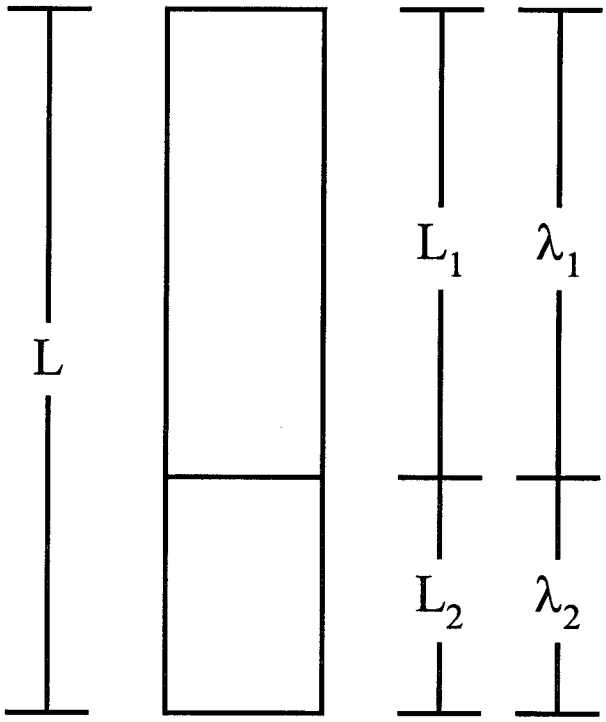

Figure 1 A series composite tensile specimen comprising two materials with different tensile moduli, E_1 and E_2, where $E_1 \leq E_2$.

From the overall elongation (ΔL) of the specimen and its initial length (L), the apparent strains (ε) were computed as

$$\varepsilon = \Delta L/L \tag{2}$$

Tensile moduli (E) were calculated as apparent stress over apparent strain:

$$E = \sigma/\varepsilon \tag{3}$$

where the strains were small and the materials were linearly elastic ($\varepsilon \leq 0.01$). Strain rates (ε') were determined from the apparent rate of elongation (v) and the initial length:

$$\varepsilon' = v/L \tag{4}$$

Series Specimens

Figure 1 shows a series composite tensile specimen. The specimen is composed of materials of different tensile moduli (E_1 and E_2), where $E_1 \leq E_2$. Both segments have the same cross-sectional area (A), but the length of each component (L_1 and L_2) can vary. For each segment, a fractional length can be defined such that

$$\lambda_1 = L_1/L \tag{5}$$

$$\lambda_2 = L_2/L \tag{6}$$

where

$$\lambda_1 + \lambda_2 = 1 \tag{7}$$

For $\lambda_1 = 1, L = L_1$. Conversely, for $\lambda_1 = 0, L = L_2$ [from eqs. (6) and (7)].

Component Stresses and Strains of Series Specimens

When load is applied, series composites deform with the same average stress in each component:

$$\sigma = \sigma_1 = \sigma_2 \tag{8}$$

However, because the materials differ in their stiffness, the individual components do not deform to the same extent. The stiffer material deforms less while softer material deforms more. The total change in length (L) is the sum of the change in each component:

$$\Delta L = \Delta L_1 + \Delta L_2 \tag{9}$$

The apparent strain (ε) in series composites is the sum of the strain in each component:

$$\varepsilon = \Delta L/L = \lambda_1\varepsilon_1 + (1 - \lambda_1)\varepsilon_2 \tag{10}$$

where

$$\varepsilon_1 = \Delta L_1/L_1 \tag{11}$$

and

$$\varepsilon_2 = \Delta L_2/L_2 \tag{12}$$

The strain in each component is related to the applied stress via their respective tensile moduli:

$$\sigma_1 = E_1\varepsilon_1 \tag{13}$$

and

$$\sigma_2 = E_2\varepsilon_2 \tag{14}$$

Combining eqs. (8), (10), (13), and (14) gives the strain in each series component in terms of the apparent strain, component moduli, and fractional length:

$$\varepsilon_1 = \varepsilon/[\lambda_1 + (1 - \lambda_1)E_1/E_2] \tag{15}$$

and

$$\varepsilon_2 = \varepsilon/[\lambda_1 E_2/E_1 + (1 - \lambda_1)] \tag{16}$$

Combining eqs. (8), (13), and (15) gives the apparent stress in series specimens in terms of the apparent strain, component modulus, and fractional length:

$$\sigma = \{E_1E_2/[\lambda_1E_2 + (1 - \lambda_1)E_1]\}\varepsilon \tag{17}$$

Apparent Modulus of the Series Composite

From eq. (17), the apparent modulus (E) of a series composite tensile specimen is

$$E = E_1E_2/[\lambda_1E_2 + (1 - \lambda_1)E_1] \tag{18}$$

Component Strain Rates and Deformation Speeds of Series Composites

Similar to strains, strain rates and deformation speeds of series composites depend on the modulus and fractional length. Strain rates of the series composites are

$$\varepsilon_1' = \varepsilon'/[\lambda_1 + (1 - \lambda_1)E_1/E_2] \tag{19}$$

and

$$\varepsilon_2' = \varepsilon'/[\lambda_1 E_2/E_1 + (1 - \lambda_1)] \tag{20}$$

Deformation speeds of the components (v_1 and v_2) differ from the apparent elongation rate (v) and can be calculated as

$$v_1 = \lambda_1 v/[\lambda_1 + (1 - \lambda_1)E_1/E_2] \tag{21}$$

and

$$v_2 = (1 - \lambda_1)v/[\lambda_1 E_2/E_1 + (1 - \lambda_1)] \tag{22}$$

Limiting Cases for Series Composites: $E_1 = E_2$

If the moduli of the two segments are equal, then eq. (15) reduces to

$$\varepsilon = \varepsilon_1 \tag{23}$$

and eq. (18) to

$$E = E_1 \tag{24}$$

Subsequently,

$$\sigma = E\varepsilon = E_1\varepsilon_1 \tag{25}$$

$E_1 \ll E_2$. If the modulus of one segment is much greater than the other, then all deformation takes place in the softer segment. The relative strain in each component can be determined by combining eqs. (13) and (14):

$$\varepsilon_2 = (E_1/E_2)\varepsilon_1 \tag{26}$$

If $E_1 \ll E_2$, eq. (26) reduces to

$$\varepsilon_2 = 0 \tag{27}$$

eq. (15) reduces to

$$\varepsilon = \lambda_1\varepsilon_1 \tag{28}$$

and the apparent modulus becomes

$$E = E_1/\lambda_1 \tag{29}$$

Thus, the apparent stress–strain behavior is determined by the softer material:

$$\sigma = E\varepsilon = (E_1/\lambda_1)\lambda_1\varepsilon_1 = E_1\varepsilon_1 \tag{30}$$

Parallel Composites

Figure 2 shows a parallel composite. As before, $E_1 \leq E_2$. Fractional cross-sectional areas are defined as

$$\alpha_1 = A_1/A \tag{31}$$

$$\alpha_2 = A_2/A \tag{32}$$

where

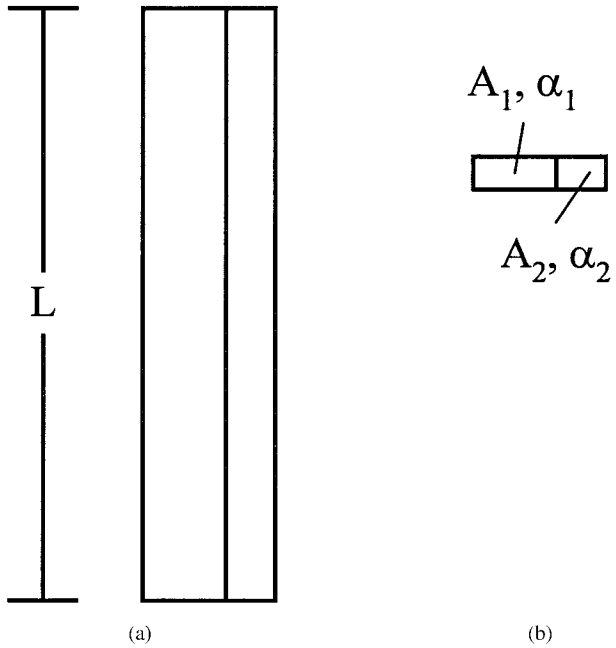

Figure 2 A parallel composite specimen comprising two materials with different tensile moduli, E_1 and E_2 where $E_1 \leq E_2$: (a) plane view; (b) cross-sectional view.

$$\alpha_1 + \alpha_2 = 1 \tag{33}$$

For $\alpha_1 = 1, A = A_1$. On the other hand, for $\alpha_1 = 0$, $A = A_2$ [from eqs. (32) and (33)].

Component Stresses and Strains of Parallel Composites

If load is applied, the composite sample deforms with the same average strain in each component:

$$\varepsilon = \varepsilon_1 = \varepsilon_2 \tag{34}$$

However, because the materials differ in their stiffness, the individual components do not require the same level of force to elongate them. The stiffer material requires more force while the softer material requires less. The total apparent force (F) is the sum of the change in each component:

$$F = F_1 + F_2 \tag{35}$$

The apparent stress in a parallel composite is the sum of the stress in each component:

$$\sigma = F/A = \alpha_1\sigma_1 + (1 - \alpha_1)\sigma_2 \tag{36}$$

where

$$\sigma_1 = F_1/A_1 \tag{37}$$

and

$$\sigma_2 = F_2/A_2 \tag{38}$$

The stress of each component is related to the applied strain via their respective tensile moduli, eqs. (13) and (14). Combining eqs. (13), (14), (34), and (36) gives the apparent stress in a parallel specimen in terms of strain, component modulus, and fractional area:

$$\sigma = [\alpha_1 E_1 + (1 - \alpha_1)E_2]\varepsilon \tag{39}$$

Apparent Modulus of the Parallel Composites

From eq. (39), the apparent modulus (E) of a parallel composite tensile specimen is

$$E = [\alpha_1 E_1 + (1 - \alpha_1)E_2] \tag{40}$$

EXPERIMENTAL

Materials

Series and parallel bimaterial composites were constructed using PC and a C fiber PEEK compound that contained <20% of the short C fiber.

Sample Preparation

Bimaterial composites were made by first molding PC tensile dogbones (ASTM Type 1), cutting them with a band saw, inserting a piece back into the mold, and then injecting C fiber PEEK.

Tensile Testing

Specimens were tested in tension at room temperature using an Instron® 5582 test machine equipped with a 100 kN static load cell and an extensometer (ASTM D638). The gauge length of the test machine was set at 115 mm. For series composites, specimens were clamped such that the interface was equidistant from each clamp and then the extensometer was positioned such that $\lambda_1 = 0.25$, 0.50, or 0.75. (See Fig. 1.) Most samples were pulled at $v = 5$ mm/min ($\varepsilon' = 8 \times 10^{-4}$ s^{-1}). A few monolithic specimens were tested at other speeds to determine any existing

Table I Tensile Properties of the Materials of Construction

Material	σ_y (MPa)	ε_y (mm/mm)	σ_b (MPa)	ε_b (mm/mm)	E (GPa)
PC (material 1)	61 ± 1	0.060 ± 0.001	66 ± 1	1.04 ± 0.01	2.4 ± 0.1
C fiber PEEK (material 2)	NY	NY	108 ± 1	0.017 ± 0.001	11.9 ± 0.2

NY, no yield.

rate dependence. Five specimens of each monolithic/composite type were analyzed for yield stress, yield strain, breaking stress, breaking strain, and modulus. Averages and standard deviations were calculated.

RESULTS AND DISCUSSION

Individual Components

The mechanical properties of the individual materials, summarized in Table I, agreed well with the literature values.[12,13] PC elongated about 6% before yielding with considerable necking and then failed at 104% elongation with a breaking stress of 66 MPa. As expected of a fiber-filled compound, C fiber PEEK failed at small strains without yielding. Its breaking stress was 108 MPa.

Neither material exhibited an appreciable rate dependence for the test speeds employed here. Strains and moduli remained constant up to v = 50 mm/min ($\varepsilon' = 8 \times 10^{-3}$ s^{-1}). With this in mind, all composite specimens were tested at a single speed, v = 5 mm/min. If these materials were rate-dependent, equivalent speeds and strains rates for monolithic and composite specimens would have been used [eqs. (19)–(22)].

Figure 3 shows typical stress–strain behavior of a PC/C fiber PEEK series composite with the extensometer centered around the interface (λ_1 = 0.50). Stresses increased linearly with elongation and the samples broke at small apparent strains without yielding. Failure occurred at or near the dogbone interface with transfer of material from one component to the other, suggesting good adhesion.

Effect of Fractional Length

Stresses in Series Composites

By changing the extensometer position, it was possible to test series composites with a range of fractional lengths (λ_1). Results are shown in Figure 4. The points are experimental data. Even though the relative length of PC was varied, stresses remained constant, eq. (8). The solid line represents an average value (40 ± 12 MPa) for C fiber PEEK. Because the interface acted as a stress raiser, breaking stresses in the series composites were significantly lower than those exhibited by the monolithic PC or C fiber PEEK.

Strains of Series Composites

Figure 5 shows the breaking strain (ε_b) versus the fractional length of PC. Points are experimental data. The modulus of C fiber PEEK was much greater than is the modulus of PC. As a result, strains were not uniform throughout the specimen—the softer PC deformed more than did its stiffer counterpart. Consequently, shifting the extensometer to increase the fractional length of PC ($\lambda_1 \rightarrow 1$) increased the breaking strain. As expected from eq. (10), the breaking strain varied linearly with the relative component length.

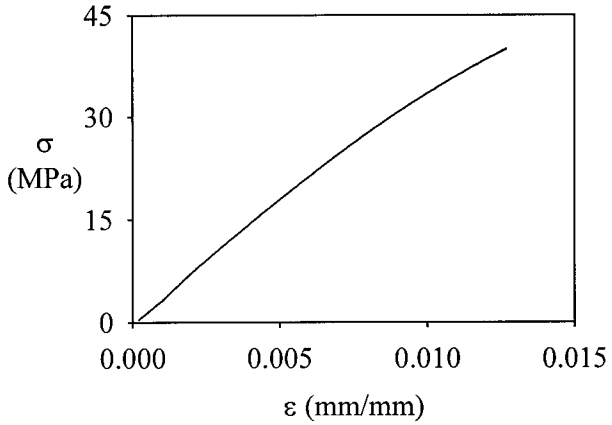

Figure 3 Stress versus strain for a series PC/C fiber PEEK composite with λ_1 = 0.5.

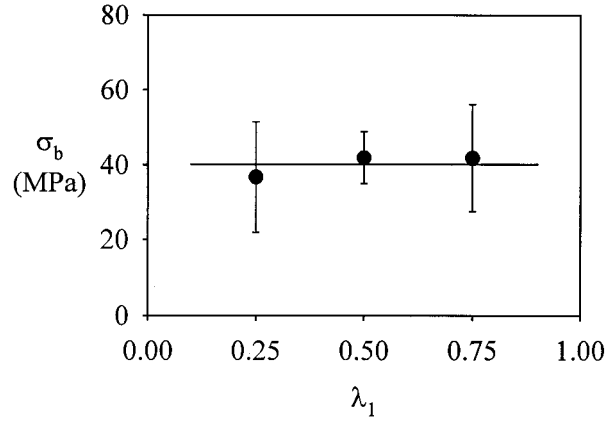

Figure 4 Breaking stress (σ_b) for series composites. Points are experimental data; the solid line represents their average.

Moduli of Series Composites

Figure 6 shows the apparent moduli for series composites where the fractional length of the PC segment was varied. The points are experimental data. The point at $\lambda_1 = 0$ represents monolithic C fiber PEEK; the point at $\lambda_1 = 1$ is for monolithic PC. Moduli of the composites were intermediate to the moduli of the individual components and decreased with PC content. Solid lines were calculated according to eq. (18). Agreement between measured and predicted values was excellent. The modulus of the PC/PC composite was included for reference. The modulus of the PC/PC composite with $\lambda_1 = 0.5$ was the same as the monolithic PC [eqs. (23)–(25)].

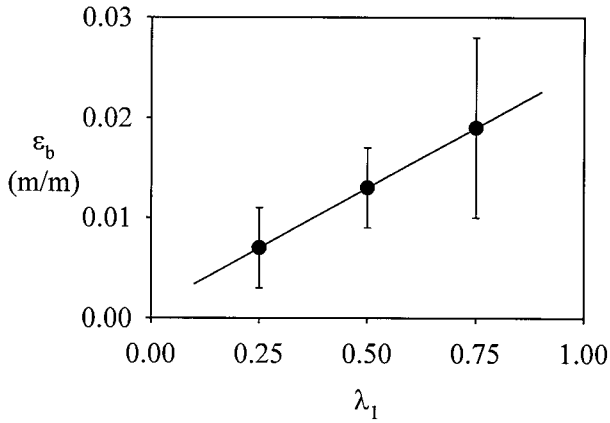

Figure 5 Breaking strain (ε_b) versus fractional length of PC (λ_1) for series composites. Points are experimental data; the solid line represents linear regression.

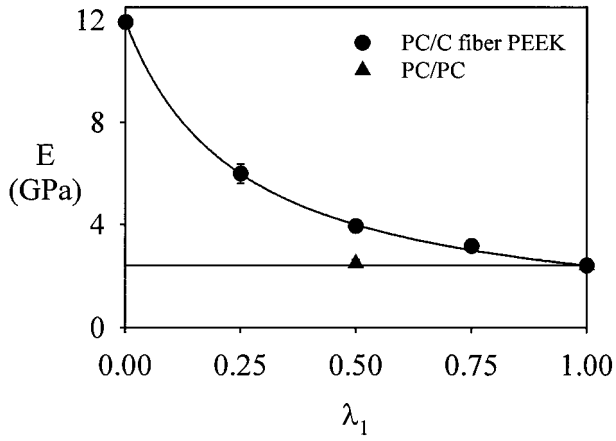

Figure 6 Apparent tensile modulus (E) versus fractional length of PC (λ_1) for series composites. The points are experimental data. The point at $\lambda_1 = 0$ represents monolithic C fiber PEEK; the point at $\lambda_1 = 1$ is for monolithic PC. Solid lines were calculated according to eq. (18).

Failure of Parallel Composites

For parallel composites, cracks initiated in C fiber PEEK and ran violently through the PC, normal to the interface and the applied load, sometimes ejecting PC fragments. No interfacial debonding was observed.

Effect of Fractional Area

Strains in Parallel Composites

Figure 7 shows the breaking strain (ε_b) versus the fractional area of PC (α_1). Points are experimental data. Breaking strains of the parallel composites were invariant, eq. (34), and equivalent to the breaking strain of the monolithic C fiber PEEK. The solid line represents an average of the breaking strains [0.018 ± 0.001 mm/mm, from C fiber PEEK ($\alpha_1 = 0$) and PC/C fiber PEEK parallel composite data].

Stresses in Parallel Composites

Figure 8 shows breaking stresses for parallel composites with different fractional areas (α_1). The points are experimental data. Increasing the relative proportion of the more compliant PC ($\alpha_1 \rightarrow 1$) caused breaking stresses to decrease linearly .

Moduli of Parallel Composites

Figure 9 shows the apparent moduli for parallel composites where the relative area of PC was

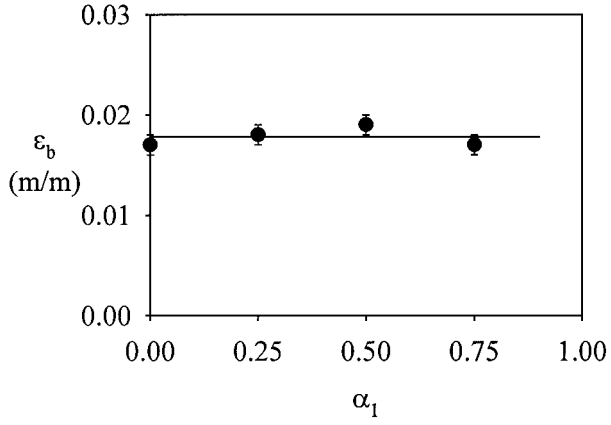

Figure 7 Breaking strain (ε_b) versus fractional area of PC (α_1) for parallel composites. Points are experimental data; the solid line represents their average.

varied. The points are experimental data. The point at $\alpha_1 = 0$ represents monolithic C fiber PEEK; the point at $\alpha_1 = 1$ is for monolithic PC. The moduli of the composites were intermediate to the moduli of the individual components, decreasing with PC content. The solid line was calculated according to eq. (40). Agreement between the measured and predicted values was good.

CONCLUSIONS

When elongated, all composites failed without yielding. Cracks always propagated normal to the applied load. Breaking stresses of the composites were considerably less than were the breaking stresses of the materials of construction, due to elevated stresses at the interface. As expected, series composites failed at or near the interface. For parallel composites, cracks initiated in C fiber PEEK and ran violently through the PC, sometimes ejecting PC fragments. No interfacial debonding was observed in the parallel composites.

For series composites, breaking stresses were independent of C fiber PEEK content, but for parallel composites, they increased with C fiber PEEK content. Conversely, breaking strains decreased with C fiber PEEK content for series composites, but were constant for parallel composites. For both series and parallel composites, stiffness increased with C fiber PEEK content.

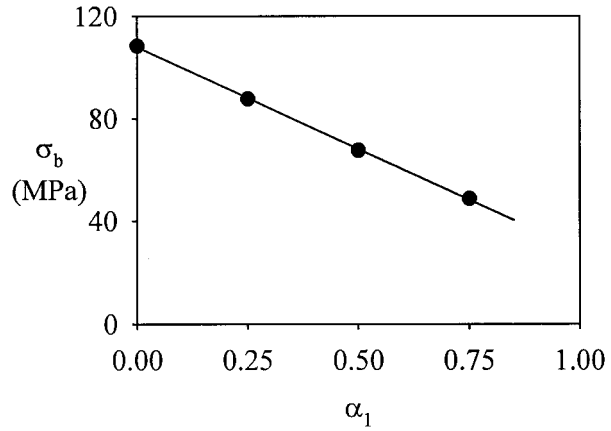

Figure 8 Breaking stress (σ_b) versus fractional area of PC (α_1) for parallel composites. Points are experimental data; the solid line is from linear regression.

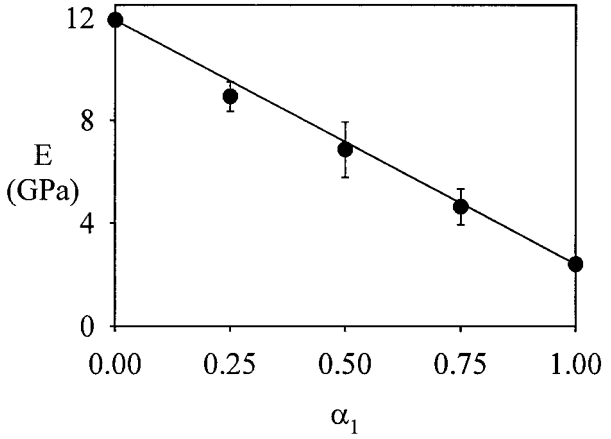

Figure 9 Apparent tensile modulus (E) versus fractional area of PC (α_1) for parallel composites. The points are experimental data. The point at $\alpha_1 = 0$ represents monolithic C fiber PEEK; the point at $\alpha_1 = 1$ is for monolithic PC. The solid line was calculated according to eq. (40).

The authors wish to thank the Entegris management for allowing the publication of this work. Also, the authors thank G. Smith and T. Raser for molding the test specimens as well as J. McPhee and B. Wold for assistance in the mechanical testing.

REFERENCES

1. De Gaspari, J. Plast Technol 1998, 44, 44–48.
2. Kausch, H. H. Advanced Thermoplastic Composites; Hanser: New York, 1993.
3. Williams, M. L. Bull Seism Soc Am 1959, 49, 199–204.
4. Sih, G. C.; Rice, J. R. J Appl Mech 1964, 31, 477–482.

5. Erdogan, F. J Appl Mech 1965, 32, 403–410.
6. Rice, J. R.; Sih, G. C. J Appl Mech 1965, 32, 418–423.
7. Hein, V. L.; Erdogan, F. Int J Fract Mech 1971, 7, 317–330.
8. Anderson, G. P.; Bennett, S. J.; DeVries, K. L. Analysis and Testing of Adhesive Bonds; Academic: New York, 1977.
9. Wu, S. Polymer Interface and Adhesion; Marcel Dekker: New York, 1982.
10. Ward, I. M. Mechanical Properties of Solid Polymers; 2nd ed.; Wiley: New York, 1983.
11. Gere, J. M.; Timoshenko, S. P. Mechanics of Materials; 2nd ed.; PWS-Kent: Boston, 1984.
12. Saechtling, H. International Plastics Handbook; 2nd ed.; Oxford University: New York, 1987.
13. International Plastics Selector; 17th ed.; D.A.T.A.: Englewood, CO, 1996; Vol. 2.